

Resveratrol attenuates doxorubicin-induced meiotic failure through inhibiting oxidative stress and apoptosis in mouse oocytes

Jun Han¹, Huarong Wang², Tuo Zhang¹, Ziqi Chen¹, Ting Zhao¹, Lin Lin¹, Guoliang Xia^{1,3}, Chao Wang¹

¹State Key Laboratory of Agrobiotechnology, College of Biological Sciences, China Agricultural University, Beijing 100193, China

²Medical College of Xiamen University, Xiamen 361005, China

³Key Laboratory of Ministry of Education for Conservation and Utilization of Special Biological Resources in the Western China, College of Life Science, Ningxia University, Yinchuan 750021, Ningxia, China

Correspondence to: Chao Wang; email: wangcam@cau.edu.cn

Keywords: doxorubicin, resveratrol, oocyte maturation, oxidative stress, DNA damage

Abbreviation: DXR: doxorubicin; RES: Resveratrol; ROS: reactive oxygen species

Received: January 18, 2020

Accepted: March 4, 2020

Published: April 30, 2020

Copyright: Han et al. This is an open-access article distributed under the terms of the Creative Commons Attribution License (CC BY 3.0), which permits unrestricted use, distribution, and reproduction in any medium, provided the original author and source are credited.

ABSTRACT

Doxorubicin (DXR), a widely used chemotherapeutic drug, has adverse effects on female fertility in young cancer patients. However, the underlying mechanisms of doxorubicin exposure on female fertility and how to prevent it have not been well studied yet. Here, mouse oocytes were employed to investigate the issues mentioned above. The results showed that doxorubicin treatment impaired oocyte meiotic maturation by destroying spindle assembly and chromosome arrangement. In addition, doxorubicin caused oxidative stress by increasing reactive oxygen species (ROS) levels. Furthermore, doxorubicin led to severe DNA damage in oocytes, which eventually induced apoptosis through DNA damage-P63-Caspase3 pathway. Conversely, resveratrol (RES) effectively improved oocyte quality by restoring spindle and chromosome configuration, reducing ROS levels and inhibiting apoptosis. In summary, our results indicate that RES can protect oocytes against doxorubicin-induced damage.

INTRODUCTION

DXR is a widely used anthracycline antibiotic, which is clinically used in the treatment of various malignant cancers, such as leukemia, lymphomas, breast, ovarian and endometrial cancer [1, 2]. However, its clinical use is limited by its dose-dependent toxicity in several organs and systems. Previous studies have shown DXR has cardiotoxicity, hepatotoxicity and reproductive toxicity [3, 4]. Early menopause, premature ovarian failure, and increasing infertility rates are the major problems for young female cancer survivors [5, 6]. In recent years, advances in cancer screening, diagnosis and therapy have markedly improved the survival rate [7]. However, most chemotherapeutic drugs are ovarian

toxic. The increasing survival rate of young cancer patients leads to more concern about their fertility state, therefore, it is important to illuminate the toxic effects and possible mechanisms of chemotherapeutic drugs on related organs and cells.

Female mammals are born with a limited number of primordial follicles and the pool of primordial follicles is a non-renewable reproductive resource for animals [8]. Previous studies in humans have shown that chemotherapeutic agents lead to a significant loss of primordial follicles and cause a reduction in ovarian reserve, which consequently shortens the reproductive lifespan of patients [9]. Also, it has been reported *in vivo* that DXR treatment causes significant decrease in

the number of primordial, primary and secondary follicles in mice. Furthermore, *in vitro* study in human has demonstrated that DXR accelerates ovarian aging [10, 11]. In ovarian granulosa cells, DXR treatment results in ROS accumulation, mitochondrial membrane potential decrease and apoptosis [12]. DXR exposure causes cell death by DNA damage and cytoplasmic fragmentation in mouse ovulated oocytes [13]. Hence, studies mentioned above suggest that DXR exerts adverse effects on ovary and that is stage and cell-type dependent. Oocyte meiotic maturation is an important event in the female reproduction process. It provides half of the genetic material and maternal components to the embryo, which is crucial for successful fertilization and subsequent embryonic development [14]. However, it remains unclear whether DXR treatment affects oocyte maturation.

RES is a natural phenolic compound and an antimicrobial produced by several plants when they are attacked by pathogens. Accumulating evidence reveals that RES scavenges free radicals and maintains the level of anti-oxidative enzymes to alleviate the damage caused by oxidative stress [15, 16]. Furthermore, it has been reported that RES protects oocyte against postovulatory aging by preventing ROS production. RES also improves the quality of oocytes *in vitro* maturation in mice and humans [17, 18]. Although previous studies have

demonstrated the adverse effects of DXR on female germ cell and the protective effects of RES on oocyte maturation, it remains unknown whether RES can protect oocytes against the damage caused by DXR treatment.

In this study, we found that DXR inhibited mouse oocyte meiotic maturation through disturbing spindle assembly and chromosome arrangement. We further demonstrated that DXR caused increased oxidative stress, DNA damage and apoptosis through DNA-damage-P63-Caspase3 pathway in mouse oocytes. On the contrary, RES effectively restored meiotic failure in DXR-treated oocytes, mitigated oxidative stress and rescued the apoptosis caused by DXR treatment.

RESULTS

RES alleviates impaired oocyte maturation in DXR-treated oocytes

Oocyte meiotic maturation is a unique asymmetric division, producing a large oocyte and a small first polar body. To assess the toxic effects of DXR on oocyte meiotic maturation, we cultured oocytes with increasing concentrations (100 nM, 200 nM, 400 nM) of DXR and calculated the rate of first polar body extrusion, which is the maker of oocyte meiotic maturation. After 12 h

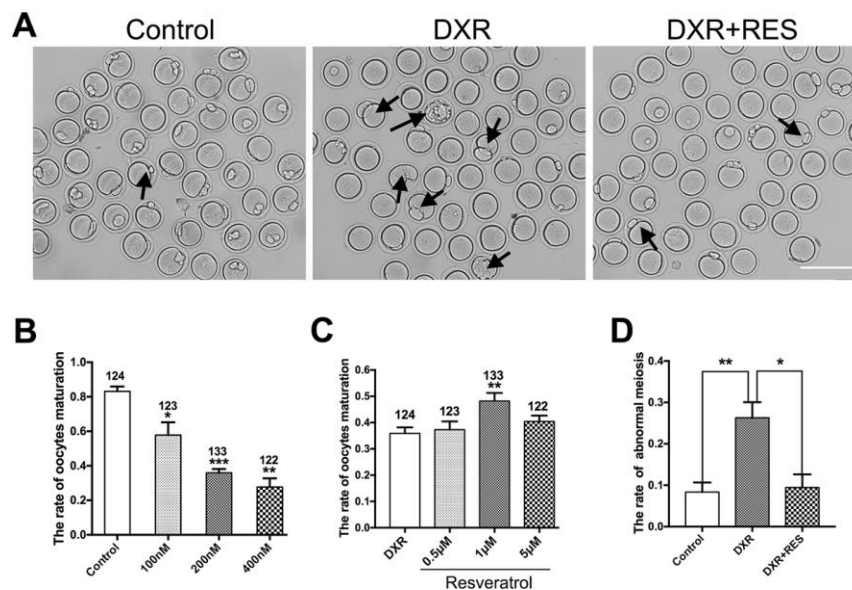


Figure 1. Effect of different concentrations of DXR and RES on oocyte meiotic maturation. (A) Microscopy images of oocytes morphologies in control, DXR treatment and RES-supplemented group, oocytes exhibited bigger first polar body (black arrowhead) after DXR treatment. Bar = 200 µm. (B) The oocyte maturation rate was recorded in control and DXR treatment groups. (C) Effect of different concentrations of RES on oocyte maturation in DXR-treated oocytes. The number of oocytes used was shown above the according column. (D) The rate of abnormal meiosis was recorded in control, DXR and RES-supplemented oocytes. All experiments were repeated at least 3 times with more than 30 oocytes examined for each experimental condition. Results were represented as means ± SEMs. * means $P < 0.05$, **means $P < 0.01$, *** means $P < 0.001$.

culture, as shown in Figure 1A, most oocytes reached the meiosis II (MII) stage ($83.21 \pm 1.61\%$, $n = 124$) in control group, however, the maturation rate in DXR treatment group significantly decreased, and some oocytes exhibited bigger first polar body, which indicated abnormal cell division. Besides, we observed that when treated oocytes with a higher concentration of DXR ($1 \mu\text{M}$), the auto-fluorescent of DXR is detectable, accumulating at the chromosome of oocyte, which indicated that DXR directly bound to oocyte chromosome to exert its toxic effects (Supplementary Figure 1). The maturation rate in 400 nM group significantly reduced to $27.63 \pm 2.91\%$ ($n = 122$) ($P < 0.01$), and it was $57.84 \pm 4.27\%$ ($n = 132$) ($P < 0.05$) in 100 nM group and $35.93 \pm 1.31\%$ ($n = 133$) ($P < 0.001$) in 200 nM group (Figure 1B). So, 200 nM was used as the final DXR treatment group in the subsequent experiments.

To examine whether RES could mitigate the impaired oocyte maturation caused by DXR treatment, we cultured oocytes with increasing concentrations of RES ($0.5 \mu\text{M}$, $1 \mu\text{M}$, $5 \mu\text{M}$) while treated with 200 nM DXR. As shown in Figure 1, $1 \mu\text{M}$ RES significantly increased the rate of oocyte maturation ($35.93 \pm 1.31\%$ vs. $48.20 \pm 1.78\%$, $P < 0.01$) and reduced the proportion of abnormal meiotic oocytes comparable to that in control group ($8.36 \pm 1.34\%$, $n = 97$ vs. $26.29 \pm 1.17\%$, $n = 103$, vs. $9.46 \pm 1.83\%$, $n = 95$, $P < 0.05$). The results herein suggested that RES partially alleviated the impaired oocyte maturation caused by DXR.

RES restores the disrupted spindle structure and chromosome alignment in DXR-treated oocytes

To investigate the reduced meiotic maturation rate in DXR treatment group, we examined spindle morphology,

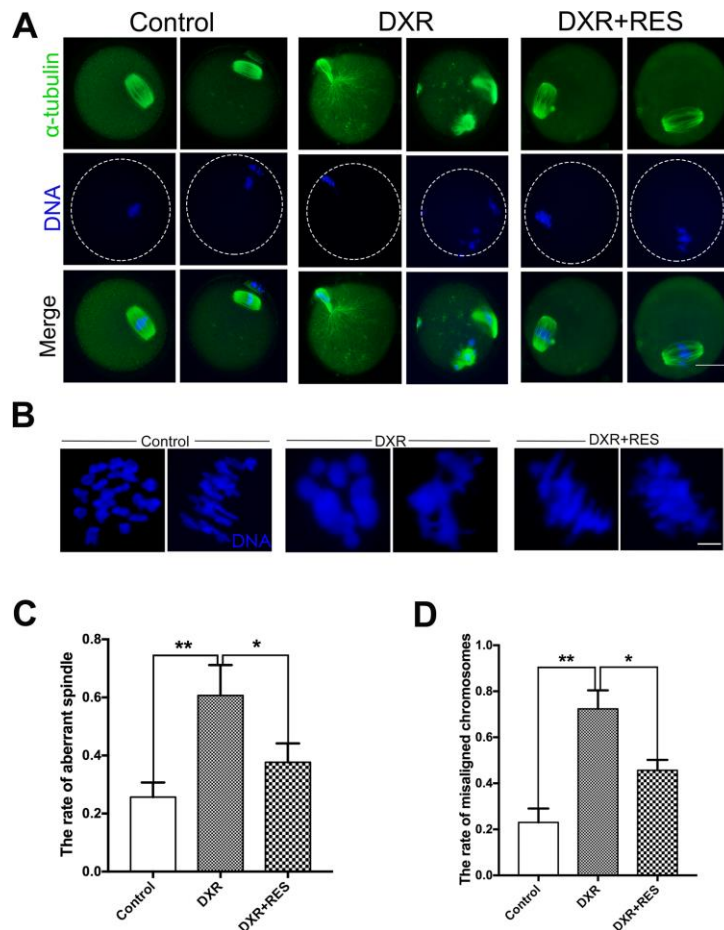


Figure 2. Effect of RES treatment on spindle morphology and chromosome alignment in DXR-treated oocytes.

Oocytes were immunolabeled with anti- α -tubulin antibody to visualize spindle and counterstained with Hoechst to observe the chromosomes. (A) Representative images of spindle morphologies and chromosome alignment in control, DXR-treated and RES-supplemented oocytes. Green, α -tubulin; blue, DNA. Bar = $20 \mu\text{m}$. (B) Representative images of chromosomes alignment in control, DXR-treated and RES-supplemented oocytes. Blue, DNA. Bar = $5 \mu\text{m}$. (C) Rate of aberrant spindle was recorded control, DXR-treated and RES-supplemented oocytes. (D) Rate of misaligned chromosomes was recorded in control, DXR-treated and RES-supplemented oocytes. All experiments were repeated at least 3 times with more than 30 oocytes examined in each experimental condition. Results were represented as means \pm SEMs. *means $P < 0.05$, **means $P < 0.01$.

actin localization and chromosome alignment in both groups. Oocytes were immunolabeled with anti- α -tubulin antibody to label the spindle and counterstained with Hoechst to observe the chromosome. As shown in Figure 2A, 2B, in control group, spindle had the typical barrel shape and chromosome well aligned on the equatorial plate, however, there was no significant difference in actin expression and localization in both groups (Supplementary Figure 2). On the contrary, spindle exhibited irregular configuration, even some aster spindle scattered in DXR treated oocytes, which might be caused by microtubule disassemble. The percentage of oocytes with aberrant spindle morphology ($60.67 \pm 6.06\%$, $n = 101$, vs. $25.67 \pm 2.91\%$, $n = 102$; $P < 0.01$) and misaligned chromosomes ($71.67 \pm 4.05\%$, vs. $23.00 \pm 3.51\%$, $P < 0.01$) were significantly increased in DXR treated group. After supplement with RES, the abnormal rates were significantly decreased ($37.67 \pm 3.76\%$, $n = 100$, $P < 0.05$, spindle; $45.67 \pm 2.6\%$, $n = 101$, $P < 0.05$, chromosome), (Figure 2C, 2D). In summary, these results suggested that RES reduced the rate of abnormal meiosis

by restoring DXR-induced spindle and chromosome disturbance.

RES mitigates oxidative stress in DXR-treated oocytes

Previous studies in different cell lines have demonstrated that ROS is one of the major toxic effects of DXR. To testify whether this was the case in oocytes as well, we detected the ROS level by DCFH-DA fluorescent probe. As shown in Figure 3A, the green signals were considerably stronger in DXR exposure oocytes. Statistical data showed that the fluorescence intensity of ROS was higher in DXR treated group compared with that in control group, but reduced in RES administration group (25 ± 3.61 , $n = 105$ vs. 72 ± 4.16 , $n = 93$ vs 40 ± 3.61 , $n = 95$, $P < 0.01$) (Figure 3B). We next assessed mRNA expression of antioxidant genes *Cat*, *Sod1*, *Sod2* and *Gpx3*. As shown in Figure 3C, the mRNA levels of *Cat*, *Sod1*, and *Gpx3* were significantly increased while the mRNA levels of *Sod2* had no significant difference

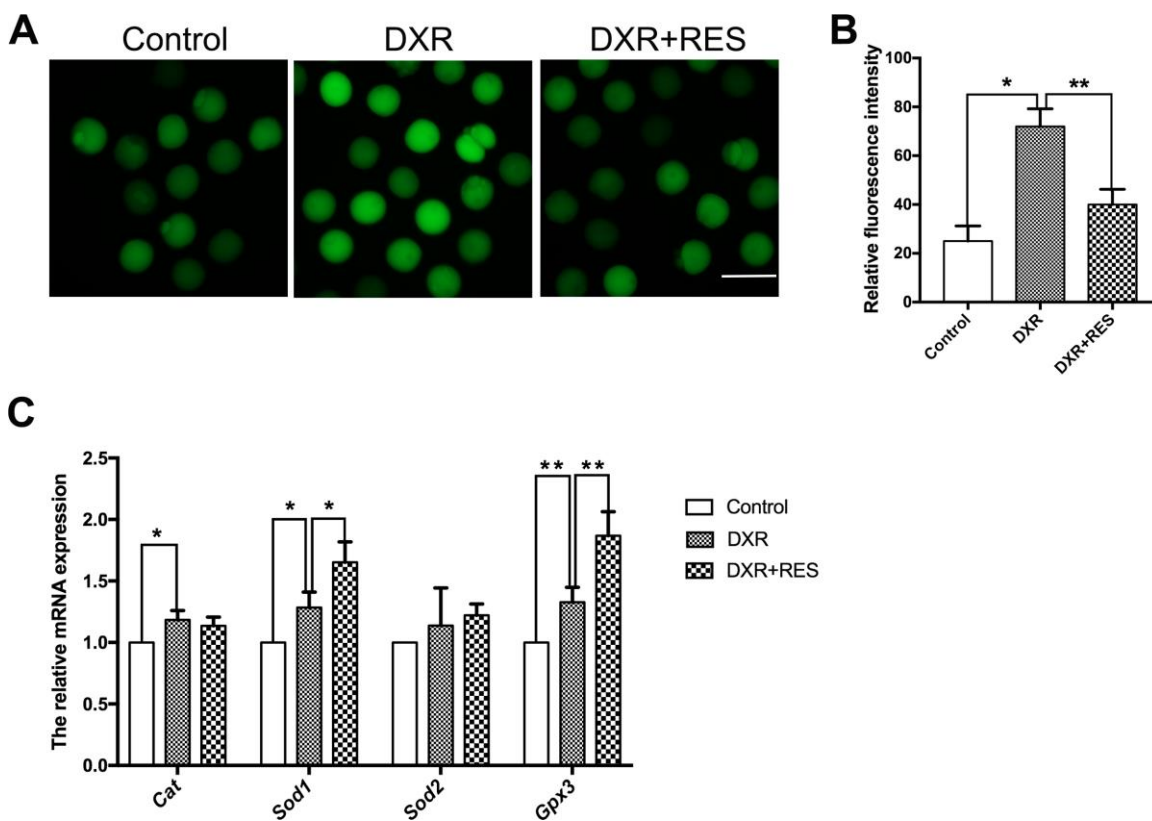


Figure 3. Effect of RES treatment on ROS levels in DXR-treated oocytes. (A) Representative images showed ROS levels in control, DXR-treated and RES-supplemented oocytes, Bar = 100 μ m. (B) The fluorescence intensity of ROS was measured in control, DXR-treated and RES-supplemented oocytes. *means $P < 0.05$, **means $P < 0.01$. (C) Relative expressions of antioxidant genes *Cat*, *Sod1*, *Sod2* and *Gpx3* mRNA levels in oocytes. β -actin was used as a housekeeping gene. *means $P < 0.05$, **means $P < 0.01$. All experiments were performed in triplicates and the data were represented as the means \pm SEM.

between the control and DXR treatment groups. Instead, RES reduced ROS levels and elevated the related antioxidant genes expression (Figure 3A–3C). Thus, these results suggested RES prevented oocytes against DXR-induced oxidative stress.

RES rescues DXR-induced apoptosis by DNA-damage-P63-Caspase3 pathway

Accumulating evidence has demonstrated that excessive ROS leads to DNA damage. Since DXR treatment caused severe oxidative stress in mouse oocytes, we wonder whether DXR treatment would cause DNA damage to oocytes. H2A histone family member X (H2AX) is one of several genes coding for histone H2A. γ -H2AX is widely used as a marker for DNA DSBs damage. We first examined γ -H2AX expression by immunofluorescence staining. As shown in Figure 4A, 4B, DXR treatment caused severe DNA damage to

oocytes, whereas RES reduced DNA damage signal to an indistinguishable level compared with that in control group according to quantitative analysis of fluorescence intensity (70.67 ± 2.96 , $n = 95$ vs. 13.00 ± 2.08 , $n = 102$ vs. 20.00 ± 2.52 , $n = 93$, $P < 0.05$). To further explore the possible pathway responsible for DXR-induced DNA damage, we then examined the protein expression of P63. Previous studies in ovarian follicles demonstrated that P63 was involved in cisplatin-induced DNA damage in mouse oocytes [19]. As shown in Figure 4C, P63 expression was markedly increased in DXR treated oocytes. Since DNA damage often triggered apoptotic pathways, we next examined active Caspase3 in both groups. As shown in Figure 4C, compared with control group, active Caspase3 expression was significantly increased in DXR-treated group, which indicated DXR treatment induced cell death in oocytes. As expected, RES rescued DXR-induced apoptosis by DNA-damage-P63-Caspase3 pathway (Figure 4A–4C).

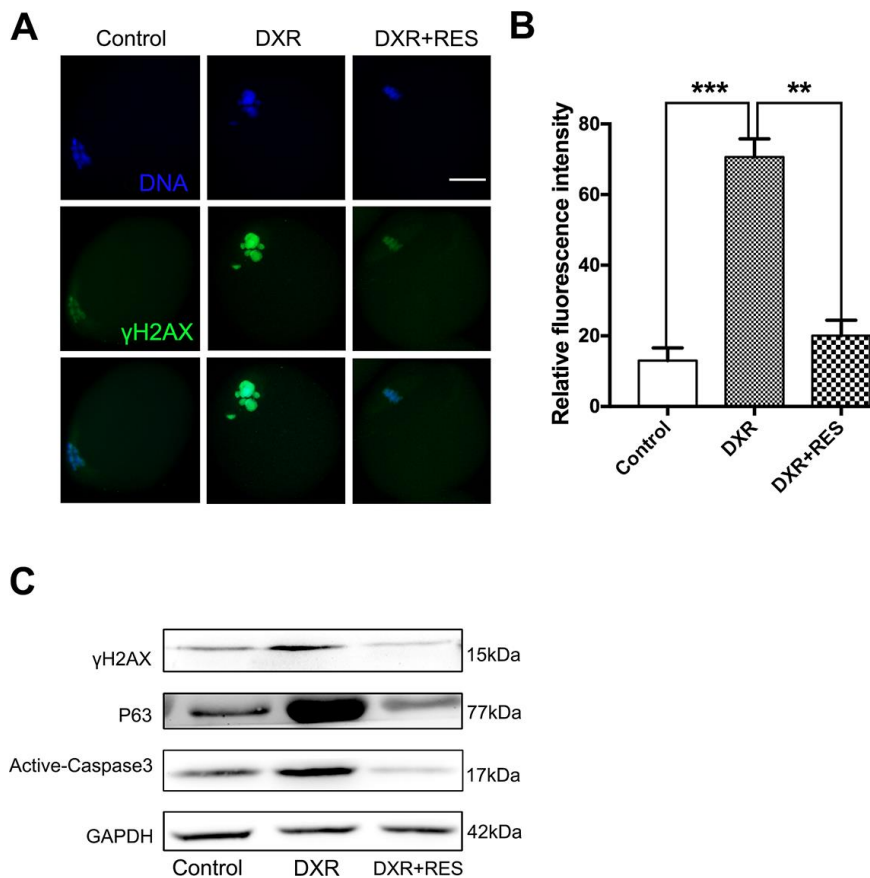


Figure 4. RES rescued DXR-induced apoptosis through DNA-damage-P63-Caspase3 pathway in mouse oocytes. (A) Representative immunofluorescence images showing the expression of γ -H2AX in mouse oocytes. Green, γ -H2AX, Blue, DNA, Bar = 20 μ m. (B) The relative immunofluorescence intensity of γ -H2AX was measured in control, DXR-treated and RES-supplemented oocytes. Experiments were repeated at least 3 times with more than 30 oocytes examined for each group. Data were presented as means \pm S.E.M of three independent experiments. **means $P < 0.01$, *** means $P < 0.001$. (C) Protein levels of γ -H2AX, P63 and Active-Caspase3 were examined by Western blotting in control, DXR-treated and RES-supplemented oocytes. GAPDH was used as a loading control. The clean backgrounds for the active-Caspase-3, γ -H2AX and GAPDH is due to the exposure.

DISCUSSION

Compromised fertility is one of the side effects of chemotherapy. Therefore, it is imperative to explore the molecular mechanisms of DXR treatment on female reproductive performance to take effective prevention methods in the clinic. Recent studies have demonstrated that RES protects oocytes from chemical agents-induced oxidative stress and apoptosis. Thus, we designed this study to investigate the possible protective role of RES on DXR-induced damage in mouse oocytes.

First, our results confirmed that DXR treatment inhibited oocyte maturation. We noticed that although some DXR-treated oocytes extruded first polar body, they exhibited bigger polar body compared with oocytes in the control group, which indicated that DXR caused abnormal cell division in mouse oocytes. Previous has shown that the enlarged first polar body is associated with impaired fertilization and embryo quality [20]. By contrast, when supplemented with RES, oocytes abnormal meiosis rate was significantly decreased. Microtubules and actin filaments are the main sources of mechanical force during oocyte meiotic maturation. DXR treatment disrupted spindle configuration and chromosome alignment while DXR treatment did not affect microfilament expression, which was similar to previous *in vivo* study using follicle as a model [21]. Meanwhile, RES administration partially restored the disrupted spindle configuration and chromosome alignment in DXR-treated oocytes. Therefore, we suggested that RES alleviated the impaired oocyte maturation caused by DXR treatment.

Several studies have shown that DXR-induced oxidative stress is one of the primary mechanisms for its toxic effects on noncancerous tissues and cells [22–24]. In physiological conditions, ROS generated during the metabolic process is a signaling molecule in female reproductive process. However, oxidative stress occurs when the equilibrium between ROS and antioxidants is disrupted [25]. In our study, after DXR treatment, ROS levels were significantly increased, which was similar to previous studies in cardiomyocyte [3, 26]. Our results also revealed that DXR upregulated the mRNA expression of antioxidant genes, which possibly due to the self-protect mechanism of oocytes. That is, oocytes may try to correct the imbalance of oxidative stress state but the increase may not high enough to resist the increase of ROS levels. Previous studies have demonstrated that elevated ROS levels disrupt spindle structure and chromosome arrangement in mouse oocytes, resulting in mismatched chromosome and causing seriously damage on oocyte quality [27, 28]. Thus, we speculated that the disorganized spindle and chromosome aberrations we observed in DXR-treated

oocytes might be caused by oxidative stress, which would ultimately inhibit oocyte maturation and reduce oocyte developmental competence.

RES is an effective antioxidant regulating the related antioxidant enzymes to protect cell against oxidative damage [15]. Notably, our results showed that RES significantly reduced ROS levels, increased the expression of antioxidant enzymes genes and alleviated the oxidative stress caused by DXR. However, RES failed to rescue the mRNA expression of *Gpx3*. The possible reason was that RES protected oocytes from DXR-induced oxidative stress by improving mitochondrial function or increasing the activity of antioxidant enzymes as reported in previous studies [29, 30]. Thus, we demonstrated that RES could improve oocyte quality through reducing oxidative damage.

DXR administration causes DNA damage in different cell types in mouse ovary and human primordial follicle [11, 13, 31], which suggests that DNA damage might be a universal mechanism responsible for its toxic effects. Consistent with these studies, our results also showed that DNA damage was markedly increased after DXR treatment. P63 plays essential roles in mediating DNA damage-induced cell death during meiotic arrest and P63 is activated when oocytes are exposed to irradiation or chemotherapeutic drug cisplatin in primordial follicles [19, 32, 33]. Our results showed that P63 expression was increased significantly after DXR treatment, which was in agreement with former studies in primordial follicles. Besides, it is well documented that extensive DNA damage triggers apoptosis in the context of DXR-induced ovarian injury [13, 31, 34]. In accordance with these studies, DXR led to increased active-Caspase3 expression in oocytes in this study. In contrast, RES attenuated DXR-induced damage through DNA-damage-P63-Caspase3 pathway.

In summary, this study shows that RES restores meiotic failure in DXR-treated oocytes by reducing ROS levels and apoptosis. These findings contribute in several ways to our understanding of DXR-induced injury to oocyte maturation and might be assistance to female fertility preservation in the clinic. However, the safety and effectiveness of RES need further investigation.

MATERIALS AND METHODS

Animals

CD-1 female mice (21-23 days old) were purchased from the Laboratory Animal Center of the Institute of Genetics and Developmental Biology (Beijing, China). All procedures were approved by the Animal Care and

Use Committee of China Agricultural University and were performed following the Animal Research Institute Committee guidelines. Mice were raised in a temperature and light-controlled room, water and food were feed *ad libitum*.

Oocyte collection and culture

Immature female CD-1 mice were killed by cervical dislocation to collect ovaries. Germinal vesicle intact oocytes were picked with a pipetted tube, each group contains at least 30 oocytes, washed several times in M2 medium, then cultured under mineral oil in M16 medium h at 37°C in 5% CO₂ atmosphere.

Reagents and antibodies

Doxorubicin hydrochloride and resveratrol were purchased from J&K Chemical Ltd. (Shanghai, China). Throughout this paper, the abbreviation DXR and RES were used to refer to doxorubicin hydrochloride and resveratrol respectively. DXR and RES were dissolved in DMSO, then diluted to the corresponding working concentrations, with the final concentration of DMSO not more than 0.1% of the culture medium. Concentrations range of doxorubicin in the study were determined from the relevant plasma level (50-200 nM) in cancer patients [35]. Finally, 200 nM was chosen as the final dosage in the following experiments.

Mouse anti- α -tubulin-FITC antibody (#F2168) was purchased Sigma-Aldrich (MA, USA); rabbit polyclonal anti- γ -H2AX antibody (#NB100-2280) was purchased from Novus (CO, USA), rabbit polyclonal anti-P63 antibody (#BS1279) was purchased from Bioworld (MO, USA), Rabbit polyclonal anti-active-Caspase3 antibody was purchased from Beyotime, (Shanghai, China). Alexa Fluor 488 goat anti-rabbit antibody, Alexa Fluor 594 goat anti-mouse antibody were from Invitrogen (CA, USA).

Immunofluorescence

Oocytes were fixed 30 min in 4% paraformaldehyde, then permeabilized with 0.5% Triton X-100 for 20 min, and blocked 1 h in blocking buffer (PBS containing 1% BSA) at room temperature, oocytes were then probed with different primary antibodies (1:400 for anti- α -tubulin-FITC; 5 μ g/ml Phalloidin-TRITC; 1:200 for γ -H2AX) at 4°C overnight, after extensive washing, oocytes were then stained with the corresponding secondary antibodies. Finally, oocytes were stained with Hoechst for 10 min to visualize the DNA, then transfer oocytes to a glass slide. The slides were examined and photographed using Nikon Eclipse 80i digital fluorescence microscopy.

The fluorescence intensity was assessed using Image J software (NIH). Samples from different groups were mounted on the same glass slide and scanned with the same parameters of fluorescence microscopy.

Analysis of intracellular ROS generation

Intracellular ROS levels were measured by detecting ROS as green fluorescent signals of DCFH diacetate (DCHFDA; Beyotime Biotechnology, Shanghai, China). After 9 h culture, oocytes from both groups were incubated at 37 °C for 30 min in D-PBS that contained 10 μ M DCHFDA. Then, the oocytes were washed 3 times with D-PBS and placed on glass slides and covered with coverslips. After that, each sample was observed immediately under a Nikon fluorescent microscope with the same scan settings.

Western blotting analysis

At least 100 oocytes were collected in each group, dissolved in SDS sample buffer then boiled at 100°C for 10 min. Protein lysates were separated by SDS-PAGE and electrophoretically transferred to PVDF membranes (Millipore, MA, USA). The membranes were blocked in Tris-buffered saline containing 0.1% Tween 20 and 5% no fat dry milk for 1 hour, then probed with primary antibodies, overnight at 4°C. After several times washing, the membranes were incubated with a horseradish peroxidase-linked secondary antibody. Finally, bands on the membranes were detected using the Super-Signal West Pico chemiluminescent detection system (Prod 34080, Thermo, USA).

RNA extraction and quantitative real-time RT-PCR

RNA was extracted from at least 150 oocytes for different groups using Trizol Reagent according to the manufacturer's protocol. Quantitative PCR was performed on a Light Cycler instrument (Roche, Mannheim, Germany). Gene expression changes were analyzed by the 2^{- $\Delta\Delta$ Ct} method and normalized with β -actin. The primers used for testing genes are listed in Supplementary Table 1.

Statistical analysis

Each experiment repeated at least 3 times with independent samples. Data are presented as means \pm SEMs and analyzed by one-way ANOVA. *P* value < 0.05 was considered significant.

AUTHOR CONTRIBUTIONS

J.H. and C.W. designed the research. J.H., H.R.W., T.Z., L.L. and T.Z. performed the experiments; J.H.

and C.W. analyzed the data; Y.M. and B.X. wrote the article. All authors read and approved the final manuscript.

CONFLICTS OF INTEREST

The authors have no conflict of interest to declare.

FUNDING

This work was supported by grants from the National Key Research and Developmental Program of China (2018YFC1003800 to C.W.; 2018YFC1003700 and 2017YFC1001100 to G.X.); National Natural Science Foundation of China (31872792 to C.W., 31371448 and 31571540 to G.X.); Project of State Key Laboratory of Agrobiotechnology (2016SKLAB-1 to G.X.); Institution of Higher Education Projects of Building First-class Discipline Construction in Ningxia Region (Biology) (NXYLXK2017B05) to G.X.

REFERENCES

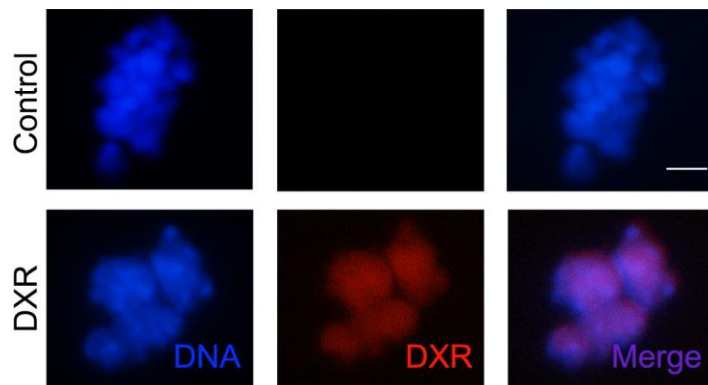
1. Paik S, Bryant J, Park C, Fisher B, Tan-Chiu E, Hyams D, Fisher ER, Lippman ME, Wickerham DL, Wolmark N. erbB-2 and response to doxorubicin in patients with axillary lymph node-positive, hormone receptor-negative breast cancer. *J Natl Cancer Inst.* 1998; 90:1361–70. <https://doi.org/10.1093/jnci/90.18.1361> PMID:9747867
2. Blum RH, Carter SK. Adriamycin. A new anticancer drug with significant clinical activity. *Ann Intern Med.* 1974; 80:249–59. <https://doi.org/10.7326/0003-4819-80-2-249> PMID:4590654
3. Zhang S, Liu X, Bawa-Khalfe T, Lu LS, Lyu YL, Liu LF, Yeh ET. Identification of the molecular basis of doxorubicin-induced cardiotoxicity. *Nat Med.* 2012; 18:1639–42. <https://doi.org/10.1038/nm.2919> PMID:23104132
4. Damodar G, Smitha T, Gopinath S, Vijayakumar S, Rao Y. An evaluation of hepatotoxicity in breast cancer patients receiving injection Doxorubicin. *Ann Med Health Sci Res.* 2014; 4:74–79. <https://doi.org/10.4103/2141-9248.126619> PMID:24669335
5. Morgan S, Anderson RA, Gourley C, Wallace WH, Spears N. How do chemotherapeutic agents damage the ovary? *Hum Reprod Update.* 2012; 18:525–35. <https://doi.org/10.1093/humupd/dms022> PMID:22647504
6. Tschudin S, Bitzer J. Psychological aspects of fertility preservation in men and women affected by cancer and other life-threatening diseases. *Hum Reprod Update.* 2009; 15:587–97. <https://doi.org/10.1093/humupd/dmp015> PMID:19433413
7. Siegel RL, Miller KD, Jemal A. Cancer statistics, 2016. *CA Cancer J Clin.* 2016; 66:7–30. <https://doi.org/10.3322/caac.21332> PMID:26742998
8. Richards JS, Pangas SA. The ovary: basic biology and clinical implications. *J Clin Invest.* 2010; 120:963–72. <https://doi.org/10.1172/JCI41350> PMID:20364094
9. Oktem O, Oktay K. Quantitative assessment of the impact of chemotherapy on ovarian follicle reserve and stromal function. *Cancer.* 2007; 110:2222–29. <https://doi.org/10.1002/cncr.23071> PMID:17932880
10. Ben-Aharon I, Bar-Joseph H, Tzarfaty G, Kuchinsky L, Rizel S, Stemmer SM, Shalgi R. Doxorubicin-induced ovarian toxicity. *Reprod Biol Endocrinol.* 2010; 8:20. <https://doi.org/10.1186/1477-7827-8-20> PMID:20202194
11. Soleimani R, Heytens E, Darzynkiewicz Z, Oktay K. Mechanisms of chemotherapy-induced human ovarian aging: double strand DNA breaks and microvascular compromise. *Aging (Albany NY).* 2011; 3:782–93. <https://doi.org/10.18632/aging.100363> PMID:21869459
12. Zhang T, He WH, Feng LL, Huang HG. Effect of doxorubicin-induced ovarian toxicity on mouse ovarian granulosa cells. *Regul Toxicol Pharmacol.* 2017; 86:1–10. <https://doi.org/10.1016/j.yrtph.2017.02.012> PMID:28219713
13. Jurisicova A, Lee HJ, D’Estaing SG, Tilly J, Perez GI. Molecular requirements for doxorubicin-mediated death in murine oocytes. *Cell Death Differ.* 2006; 13:1466–74. <https://doi.org/10.1038/sj.cdd.4401819> PMID:16439991
14. Sun SC, Kim NH. Molecular mechanisms of asymmetric division in oocytes. *Microsc Microanal.* 2013; 19:883–97. <https://doi.org/10.1017/S1431927613001566> PMID:23764118
15. Yen GC, Duh PD, Lin CW. Effects of resveratrol and 4-hexylresorcinol on hydrogen peroxide-induced oxidative DNA damage in human lymphocytes. *Free Radic Res.* 2003; 37:509–14. <https://doi.org/10.1080/1071576031000083099> PMID:12797471
16. Rege SD, Kumar S, Wilson DN, Tamura L, Geetha T, Mathews ST, Huggins KW, Broderick TL, Babu JR. Resveratrol protects the brain of obese mice from

- oxidative damage. *Oxid Med Cell Longev*. 2013; 2013:419092.
<https://doi.org/10.1155/2013/419092>
PMID:24163719
17. Liang QX, Lin YH, Zhang CH, Sun HM, Zhou L, Schatten H, Sun QY, Qian WP. Resveratrol increases resistance of mouse oocytes to postovulatory aging *in vivo*. *Aging (Albany NY)*. 2018; 10:1586–96.
<https://doi.org/10.18632/aging.101494>
PMID:30036861
18. Liu MJ, Sun AG, Zhao SG, Liu H, Ma SY, Li M, Huai YX, Zhao H, Liu HB. Resveratrol improves *in vitro* maturation of oocytes in aged mice and humans. *Fertil Steril*. 2018; 109:900–07.
<https://doi.org/10.1016/j.fertnstert.2018.01.020>
PMID:29778389
19. Gonfloni S, Di Tella L, Caldarola S, Cannata SM, Klinger FG, Di Bartolomeo C, Mattei M, Candi E, De Felici M, Melino G, Cesareni G. Inhibition of the c-Abl-TAp63 pathway protects mouse oocytes from chemotherapy-induced death. *Nat Med*. 2009; 15:1179–85.
<https://doi.org/10.1038/nm.2033>
PMID:19783996
20. Ebner T, Yaman C, Moser M, Sommergruber M, Feichtinger O, Tews G. Prognostic value of first polar body morphology on fertilization rate and embryo quality in intracytoplasmic sperm injection. *Hum Reprod*. 2000; 15:427–30.
<https://doi.org/10.1093/humrep/15.2.427>
PMID:10655316
21. Xiao S, Zhang J, Liu M, Iwahata H, Rogers HB, Woodruff TK. Doxorubicin Has Dose-Dependent Toxicity on Mouse Ovarian Follicle Development, Hormone Secretion, and Oocyte Maturation. *Toxicol Sci*. 2017; 157:320–29.
<https://doi.org/10.1093/toxsci/kfx047> PMID:28329872
22. Gilliam LA, Moylan JS, Patterson EW, Smith JD, Wilson AS, Rabhani Z, Reid MB. Doxorubicin acts via mitochondrial ROS to stimulate catabolism in C2C12 myotubes. *Am J Physiol Cell Physiol*. 2012; 302:C195–202.
<https://doi.org/10.1152/ajpcell.00217.2011>
PMID:21940668
23. Fu Z, Guo J, Jing L, Li R, Zhang T, Peng S. Enhanced toxicity and ROS generation by doxorubicin in primary cultures of cardiomyocytes from neonatal metallothionein-I/II null mice. *Toxicol In Vitro*. 2010; 24:1584–91.
<https://doi.org/10.1016/j.tiv.2010.06.009>
PMID:20600803
24. Songbo M, Lang H, Xinyong C, Bin X, Ping Z, Liang S. Oxidative stress injury in doxorubicin-induced cardiotoxicity. *Toxicol Lett*. 2019; 307:41–48.
<https://doi.org/10.1016/j.toxlet.2019.02.013>
PMID:30817977
25. Kala M, Shaikh MV, Nivsarkar M. Equilibrium between anti-oxidants and reactive oxygen species: a requisite for oocyte development and maturation. *Reprod Med Biol*. 2016; 16:28–35.
<https://doi.org/10.1002/rmb2.12013>
PMID:29259447
26. Ichikawa Y, Ghanefar M, Bayeva M, Wu R, Khechaduri A, Naga Prasad SV, Mutharasan RK, Naik TJ, Ardehali H. Cardiotoxicity of doxorubicin is mediated through mitochondrial iron accumulation. *J Clin Invest*. 2014; 124:617–30.
<https://doi.org/10.1172/JCI72931> PMID:24382354
27. Choi WJ, Banerjee J, Falcone T, Bena J, Agarwal A, Sharma RK. Oxidative stress and tumor necrosis factor-alpha-induced alterations in metaphase II mouse oocyte spindle structure. *Fertil Steril*. 2007 (Suppl); 88:1220–31.
<https://doi.org/10.1016/j.fertnstert.2007.02.067>
PMID:17601599
28. Tamura H, Takasaki A, Miwa I, Taniguchi K, Maekawa R, Asada H, Taketani T, Matsuoka A, Yamagata Y, Shimamura K, Morioka H, Ishikawa H, Reiter RJ, Sugino N. Oxidative stress impairs oocyte quality and melatonin protects oocytes from free radical damage and improves fertilization rate. *J Pineal Res*. 2008; 44:280–87.
<https://doi.org/10.1111/j.1600-079X.2007.00524.x>
PMID:18339123
29. Lagouge M, Argmann C, Gerhart-Hines Z, Meziane H, Lerin C, Daussin F, Messadeq N, Milne J, Lambert P, Elliott P, Geny B, Laakso M, Puigserver P, Auwerx J. Resveratrol improves mitochondrial function and protects against metabolic disease by activating SIRT1 and PGC-1alpha. *Cell*. 2006; 127:1109–22.
<https://doi.org/10.1016/j.cell.2006.11.013>
PMID:17112576
30. Mokni M, Elkahoui S, Limam F, Amri M, Aouani E. Effect of resveratrol on antioxidant enzyme activities in the brain of healthy rat. *Neurochem Res*. 2007; 32:981–87.
<https://doi.org/10.1007/s11064-006-9255-z>
PMID:17401679
31. Roti Roti EC, Leisman SK, Abbott DH, Salih SM. Acute doxorubicin insult in the mouse ovary is cell- and follicle-type dependent. *PLoS One*. 2012; 7:e42293.
<https://doi.org/10.1371/journal.pone.0042293>
PMID:22876313
32. Suh EK, Yang A, Kettenbach A, Bamberger C, Michaelis AH, Zhu Z, Elvin JA, Bronson RT, Crum CP, McKeon F.

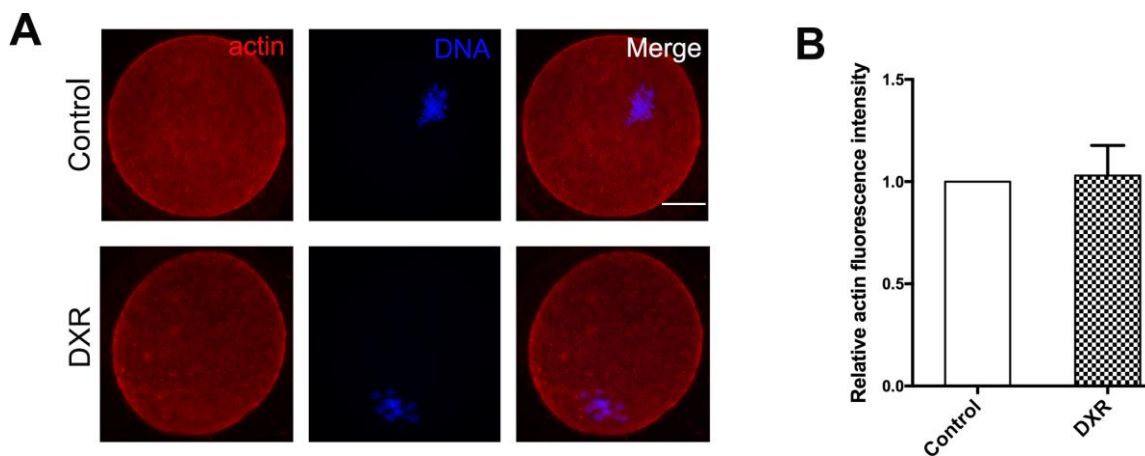
- p63 protects the female germ line during meiotic arrest. *Nature*. 2006; 444:624–28.
<https://doi.org/10.1038/nature05337>
PMID:17122775
33. Livera G, Petre-Lazar B, Guerquin MJ, Trautmann E, Coffigny H, Habert R. p63 null mutation protects mouse oocytes from radio-induced apoptosis. *Reproduction*. 2008; 135:3–12.
<https://doi.org/10.1530/REP-07-0054>
PMID:18159078
34. Wang Y, Liu M, Johnson SB, Yuan G, Arriba AK, Zubizarreta ME, Chatterjee S, Nagarkatti M, Nagarkatti P, Xiao S. Doxorubicin obliterates mouse ovarian reserve through both primordial follicle atresia and overactivation. *Toxicol Appl Pharmacol*. 2019; 381:114714.
<https://doi.org/10.1016/j.taap.2019.114714>
PMID:31437492
35. Bar-Joseph H, Ben-Aharon I, Rizel S, Stemmer SM, Tzabari M, Shalgi R. Doxorubicin-induced apoptosis in germinal vesicle (GV) oocytes. *Reprod Toxicol*. 2010; 30:566–72.
<https://doi.org/10.1016/j.reprotox.2010.07.003>
PMID:20656019

SUPPLEMENTARY MATERIALS

Supplementary Figures



Supplementary Figure 1. Co-localization of DXR and oocyte chromosomes. DXR-treated oocytes showed positive fluorescent signal and co-localized with DNA in oocytes. Blue, DNA; red, DXR.



Supplementary Figure 2. DXR exposure did not affect actin expression in mouse oocytes. (A) Representative images of actin localization in control and DXR-treated oocytes. (B) The fluorescence intensity of actin was measured in control and DXR-treated oocytes. Results were presented as means \pm SEMs of at least 3 independent experiments with more than 30 oocytes examined for group. Bar = 20 μ m.

Supplementary Table

Supplementary Table 1. Primer sequences for qRT-PCR.

	Forward	Reverse
<i>Cat</i>	ACCAAATACTCCAAGGCAAAGGT	CAAACCCACGAGGGTCCCGA
<i>Sod1</i>	GCTGTACCAGTGCAGGTCCTCA	CATTTCACCTTTGCCCAAGTC
<i>Sod2</i>	AAAGCGGTGTGCGTGCTGAA	CAGGTCTCCAACATGCCTCT
<i>Gpx3</i>	CCTCAAGTACGTCCGACCTG	CAATGTCGTTGCGGCACACC
<i>β-actin</i>	TTGTTACCAACTGGGACG	GGCATAGAGGTCTTTACGG